Automatic Time-Frequency Analysis of MRPs for Mind-controlled Mechatronic Devices

Daniela De Venuto, Giovanni Mezzina
Dept. of Electrical and Information Engineering
Politecnico di Bari
Bari, 70125, Italy
{daniela.devenuto, giovanni.mezzina}@poliba.it

***Abstract*— This paper describes the design, implementation and in vivo test of a novel Brain Computer Interface (BCI) for the mechatronic devices control. The method exploits electroencephalogram acquisitions (EEG), and specifically the Movement Related Potentials (MRPs) (i.e., μ and β rhythms), to actuate the user intention on the mechatronic device. The EEG data are collected by only five wireless smart electrodes positioned on the central and parietal cortex area. The acquired data are analyzed by an innovative single-trial classification algorithm that, with respect to the current state of the art, strongly reduces the training time (Minimum: ~1 h, reached: 10 min), as well as the acquisition time - after stimulus - for a reliable classification (Typical: 4-8 s reached: 2 s). As first step, the algorithm performs an EEG time-frequency analysis in the selected bands, making the data suitable for further computations. The implemented machine learning (ML) stage consists of: (i) dimensionality reduction; (ii) statistical inference-based features extraction (FE); (iii) classification model selection. It is also proposed a dedicated algorithm, the MLE-RIDE, for the dimensionality reduction that, jointly with statistical analyses, digitalize the μ and β rhythms, performing the features extraction. Finally, the best support vector machine (SVM) model is selected and used in the on-line classification. As proof of concept, two mechatronic devices have been brain-controlled by using the proposed BCI algorithm: a three-finger robotic hand and an acrylic prototype car. The experimental results, obtained with data from 3 subjects (aged 26±1), showed an accuracy on human will wireless detection of 87.4%, in the real-time binary discrimination, with 33.7ms of computation times.**

Keywords— BCI, MRP, Classification, SVM, Simulink

I. INTRODUCTION

The worldwide impact of neuro-degenerative diseases, bringing losses of motor neurons and, then, the partial or complete paralysis (e.g. in amyotrophic lateral sclerosis), led several research groups in developing Brain Computer Interfaces (BCI) to enhance the life quality of these patients. Indeed, the BCIs, in their most general definition, allow discriminating the user intentions by "mind reading" from electroencephalogram (EEG) sequences.

They are not a clinical prerogative but found a huge range of ordinary life applications, such as wheelchairs or cars driving [1, 2], communication assisting [3], prosthetic solutions [4], gaming [5] and ambient assisted living [6].

Nevertheless, in a non-invasive BCI framework, three main issues must be solved [7]. The first issue concerns the identification of the right clinical protocol to be submitted to the subject, in order to modulate his brain response, making it readable by the BCI. The second issue is related to the choice of the brain activity pattern (BAP). The BAP must be capable to convey the subject's intention to the computer. The last trend in the research area concerns the single-trial EEG classification improvement. Indeed, achieving high single-trial accuracy means creating fast, robust and easy to be handleable BCIs [7]. The BAPs that allow to realize a reliable single trial classification are typically: the event related potentials (ERPs), the slow cortical potentials (SCP), the event-related (de-) synchronization potentials (ERD/ERS), the steady state visual potentials (SSVP) and the sensorimotor rhythms (SMR) [7]. Several single-trial based BCI were proposed by the state of the art and they have been summarized in the Table I [8-11]. Some noteworthy solutions are compared with the proposed work in terms of: chosen BAP, FE and classification methods, mean accuracy, EEG trial length after stimulation (AS), number of subjects involved in the test, data rate (commands/min) and number of available choices.

In this context, the paper proposes a novel BCI methodology able to reduce the training time (from a minimum of ~1h to about 10 min) and the EEG trials length needed for accurate BAP recognition (from 4s or 8s to 2s with only 1s after the stimulation), remaining competitive with the state of the art in term of classification accuracy.

This paper fully investigates the evolution of two movement related potentials (MRPs), the μ and β rhythms, considering their time-frequency responses during several stimulation protocols. The implemented algorithm analyzes the EEGs, from 5 smart electrodes, in the time-frequency domain, considering the frequency bands of interest. In the machine learning (ML) phase, the data to be evaluated are submitted to a first dimensionality reduction through a dedicated algorithm,

TABLE I. COMPARISON WITH THE STATE OF THE ART

System	[8]	[9]	[10]	[11]	Our work
BAP	SCP	ERD/ERS	ERPs	Oscillatory Rhythms	MRPs
Methods	Imagery Modulation + Threshold	Standard AR + ANN	LLP Algorithm Unsupervised Method	Motor Imagery + CVA+ Gaussian	MLE-RIDE + Statistics+ SVM
# Electr.	32	56	31	16	5
Mean Accuracy (%)	85.6 % *(offline)*	83.6% (*pseudo real-time*)	90.2% (*pseudo real-time*)	86.2% *(online)*	87% *(online)*
Training time	~50 h	~ 4 h	~ 4 h	2 weeks	~ 10 min
EEG trial length AS	4 s	8 s	17 s	1 s	1 s
Data rate (com/min)	2	6	2.4	2	8
# Choices	2	3	24	2	2
Dataset (subjects)	2	3	13	10	3

*AR: Autoregressive Coefficients, ANN: Artificial Neural Network, LLP: learning label proportions, CVA: Canonical Variate Analysis

named MLE-RIDE. It extracts the residuals-based averages for each channel and available movement, excluding from further computing the less descriptive MRPs waveforms. Then, the BCI realizes a digitalization on the preserved data by using statistical inference-based thresholds. Formally, the resulting digitized signal represents the features to be classified.
The paper evaluates several classification models for the final ML step.
As proof of concept, the commands provided by the real-time classification are sent via Bluetooth to two external mechatronic devices: a three-finger robotic hand and an acrylic prototype car. With about 10min of training and 1s AS long EEG trials, the proposed BCI can reach the 87.36% of accuracy, in a real-time binary discrimination context.
The paper is structured as follows: Sec. II describes the clinical background and the stimulation protocols used. Sec. III provides information about the overall architecture, from the ML stage to real-time classification. The Sec. IV outlines the features of the actuators used as proof of concept. Sec. V describes the experimental results and Sec. VI underlines the conclusions and further perspective.

II. Clinical Background and Stimulation Protocols

A. The Selected Brain Activity Pattern

First, Several clinical studies [12] demonstrated that during voluntary movements, a cerebral preparation process precedes activation of proper muscles sequence. For this reason, we focused on BAPs, which are specifically related to the preparation and execution of a motor command, rather than reflecting merely unspecific modulations of vigilance or attention [7, 12].
Typically, the neural preparation process starts 1 s before the muscle contraction and it is characterized, inter alia, by EEG potentials named movement-related potentials (MRPs) [12]. In this paper, we studied two highly descriptive MRPs for the BCI application: the μ-rhythms, and the β-rhythms [12, 13]. The μ-rhythm occupies a frequency band between 9 and 11 Hz and can occur up to 1 s before the movement activation. Performing a motor action suppresses this rhythm. The β-rhythm has a frequency band ranging from 12.5 to 30 Hz. This premotor cortex rhythm is responsible for muscles firing management [12]. MRPs are typically more visible in the central and early parietal cortex areas known as motor and sensory regions (Fig. 1), and specifically in the brain hemisphere opposite to the limb that performs the movement.
Finally, as stated by the author in [7], the multi-channel EEG-mapping demonstrated that some localized brain areas contribute to cerebral motor command processes, via an MRP known as Bereitschaftspotential (BP). The BP moves from 2Hz to 5Hz and in time-domain it is a negative deflection that precedes the voluntary initiation of the movement and it is clearly visible in lateral scalp positions (C3, C4) [7, 14, 15]. It is not useful to distinguish two specific actions (e.g., left or right finger movements).

B. The Stimulation Protocols

To provide a complete overview of the MRPs applicability in the BCI framework, several protocols have been carried out both in controlled and noisy environments. These tests have been designed to emphasize the movement voluntariness [16].
In the following, all the tests will be uniquely numbered. The test number can be followed by a subscript "N" if the test was carried out in a noisy environment.
Test0$_{(N)}$. The user is sitting in resting state, without interactions with other participants or staff. The system continually investigates the user brain response in the frequency band of interest. It is used as a ground truth level of voluntariness.
Test1$_{(N)}$. The user is sitting in front of a button. The user counts mentally to 5 s, then, with the prescribed hand, he pushes the button.
Test2$_{(N)}$. The user is sitting in front of a button. He randomly pushes the button with self-paced timing by using the prescribed hand.
Test3$_{(N)}$. Like the Test2, but there are no interactions with the push button. The finger movement is however permitted.
Test4$_{(N)}$. The user is sitting in front of a push button, with a buzzer in the same test environment. The buzzer is programmed to sound with a random inter-stimulus timing (from 3s to 9s). It emits two different tones to indicate that the button must be pressed with the right hand finger or with the left hand one.

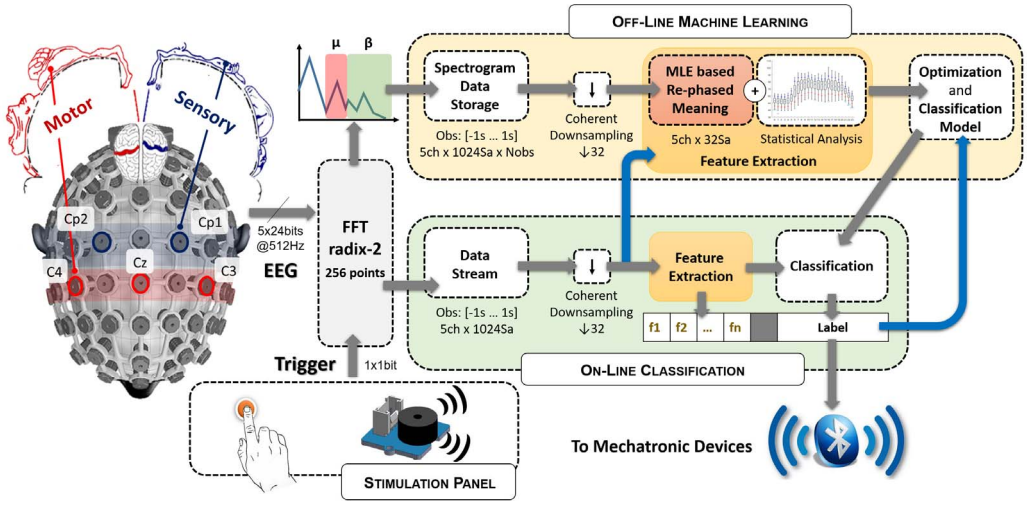

Fig.1 Overall system schematic from the acquisition to the machine learning stage, the classification model extraction and the on-line classification. The blue arrows indicate the self-adapting nature of the implemented algorithm.

Test5$_{(N)}$. The user is sitting and focuses his attention to the buzzer emitted tones. The buzzer is programmed in the same way of the Test4. When the buzzer sounds the user programs the defined movement without interacts with the switch.

III. The Overall Architecture

Fig. 1 shows a block diagram of the implemented BCI architecture from the signal acquisition to the on-line mechatronic activation. The overall architecture can be divided into five main operative units: (i) the acquisition unit; (ii) the Stimulation Panel (iii) the Off-line Machine Learning unit (iv) the On-line Classification block and (v) the Bluetooth based communication interface. The proposed system has been fully implemented in MATLAB 2017b and Simulink environments. The off-line ML processing has been entrusted to MATLAB scripting, while the EEG acquisition, the Stimulation management, the on-line features extraction (FE), the BAP classification and the commands transmission via Bluetooth, operate in *real-time* on Simulink. The Stimulation Panel consists of a tactile switch and a buzzer and it is controlled via ATMega328 P-PU programming.

A. The System Operation

The operation of the BCI can be briefly described as follows: the EEGs are acquired from a wireless headset, which collects and filters the data, sending them via Bluetooth Low Energy to a base station connected to a PC USB socket. This base station provides a set of digital inputs, which can be interfaced to external trigger signals, to synchronize them with the EEGs. The Stimulation Panel outputs are connected to them.

When new EEG samples occur, they undergo a Short Time Fourier Transform (FFT radix 2 in Fig.1) with sampling rate f_s=512samples/s and window length L_w=256 samples [17] (resolution of 2Hz). In the L_w window, the power spectrum densities of the μ and β rhythms are progressively summed. The FFT block, in fig. 1, provides two waveforms in output. The BP waveform is extracted in a similar way. The BP was studied [7, 11] to differentiate between them the resting state and the onset of the voluntary movement, without the need for external triggers, as explained in Sec II.B: Test0. BP amplitude variation has been used as trigger during the Test3.

Considering a generic test (e.g. the Test4): when the buzzer sounds and the user pushes the button, the trigger signal extracts a piece of the streamed μ and β waveforms. This temporal window is known as *trial* and consists in 2 s (1024 samples) of acquisition: 1 s before the trigger rising edge and 1s after it. In the following, the β and μ signals will be numbered the notation: "β(or μ)$_{Ch,M}$" (e.g. βC_{3R}) where *Ch* is the channel on which the MRP is evaluated and *M* is the performed movement (R: right hand, L: left hand movement). Moreover, all the β or μ signals are referenced to the respective Cz magnitude in a differential way: e.g. βC_{3R}= βC_{3R}'- βC_{ZR} and so on, with βC_{3R}' monopolar version of βC_{3R}.

During the learning stage, the trials are collected in 3D observations matrices and sent to an algorithm able to emphasized the neural potential differences when a specific movement is performed. The ML stage exploits a waveform re-phasing approach based on a residue iterative decomposition algorithm, empowered by a Maximum likelihood (MLE-RIDE) estimation algorithm. The MRPs, on specific channels, that do not ensure highly descriptive differences between right and left-hand movement are excluded from the statistical inference-based FE. This statistical study identifies some thresholds, allowing to "barcode" the selected signals. The extracted features are used to train a set of Support Vector Machines (SVM) with four different kernels. The model with the best validated accuracy is selected as the one to be implemented in the real-time discrimination context.

In the on-line classification context, the extracted trials (that are unlabeled) undergo the FE phase, coherently with the one operated in the ML stage. The features are used to feed an SVM that provides the specific command linked to the user intention. Finally, the Simulink model sends a message to a generic Bluetooth receiver (e.g. in this application, a low-cost HC-05). It manages the command to be applied on the specific mechatronic device responsible of the actuation. The tested devices (robotic hand and acrylic prototype car) are both managed in actuation by an ATMega328 P-PU board.

B. The Acquisition Unit

The acquisition unit is sketched on the left of the Fig.1 as an EEG headset with two semi-transparent area. These are the motor (red) and sensory (blue) cortex areas. The implemented multichannel sensing system consists in a 32-channel EEG headset. For this application, data from 5 EEG channels on the sensorimotor area have been wirelessly acquired: C3, Cz, C4, Cp1, Cp2. The AFz electrode is used as GND for a monopolar reading and the right ear lobe is used as reference electrode (REF) [16, 17]. EEG samples are recorded in an analog input range of ±187.5mV with 24bit resolution at 500Hz sampling rate. In the Simulink interface, the EEGs are numerically band-pass filtered between 0.5Hz and 35Hz (8th order Butterworth). Finally, an amplitude winsorizing approach completes the preprocessing, deleting - from further computing - the EEG outliers and reducing the artifacts effect.

C. The Acquisition Unit

The implemented multichannel sensing system consists in a 32-channel EEG headset. For this application, data from 5 EEG channels on the sensorimotor area have been wirelessly acquired: C3, Cz, C4, Cp1, Cp2. The AFz electrode is used as GND for a monopolar reading and the right ear lobe is used as reference electrode (REF) [16, 17]. EEG samples are recorded in an analog input range of ±187.5mV with 24bit resolution at 500Hz sampling rate. In the Simulink interface, the EEGs are numerically band-pass filtered between 0.5Hz and 35Hz (8th order Butterworth). Finally, an amplitude winsorizing approach completes the preprocessing, deleting - from further computing - the EEG outliers and reducing the artifacts effect.

D. The Off-Line Machine Learning

The first step of the ML stage is entrusted to the MLE-RIDE algorithm, which is able to extract a coherent average along a high number of observations. Usually, when this number increases, the mathematical average, in classic sense, loses of significance due to the broadening effect [18]. The MLE-RIDE is an improved version of the most used tuned-RIDE [18]. Differently from the t-RIDE that can extract only event related potentials (e.g. P300) from the background EEG, the MLE-RIDE can be used to re-phase any statistically relevant part of the signal with no limitations in applicability. Indeed, the main

differences from t-RIDE [18] concern: (i) the number of components that can be emphasized (not only one as in the t-RIDE, but up to 4 components along the trial), (ii) the latency re-phasing alignment is based on MLE and not on Woody method. It strengthens the algorithm against the inter-trial jitter error [18].

The Fig.2a shows the differences in analyzing a classic average or a re-phased one. In particular, the Fig.2a shows in solid blue line the phased mean of the βC_{3R} against a classic average in dashed blue line. It also shows in solid red line the phased mean of the βC_{3L} and the classic average (dashed line).

After the EEGs acquisition for the specific test (Sec. II.B), the MATLAB script receives two observations matrices: $\mathbf{OM_\beta}$ and $\mathbf{OM_\mu} \in \mathbb{R}^{Ch,S,No}$ with S number of samples and N_o number of observations realizing the dataset. $\mathbf{OM_\beta}$ and $\mathbf{OM_\mu}$ comprise the trials for the right-hand movements and left hand ones.

The Fig.2b shows two graphs Observation vs Trial samples: 50 trials of μ_{Cp2R} and 72 trials of μ_{Cp2L}. In these plots some differences are visible in terms of magnitude: centrally, the μ_{Cp2L} (left hand movement) is higher than μ_{Cp2R}.

Firstly, the system analyzes $\mathbf{OM_\beta}$ and $\mathbf{OM_\mu}$ extracting the phased averages of 16 signals (1 β and 1 μ for all the 4 channels and for the 2 directions): βC_{3R}, βC_{3L}, βC_{4R}, βC_{4L}, βC_{p1R}, βC_{p1L}, βC_{p2R}, βC_{p2L}, μC_{3R}, μC_{3L}, μC_{4R}, μC_{4L}, μC_{p1R}, μC_{p1L}, μC_{p2R}, μC_{p2L}.

Then, it identifies the most different waveforms with reference to the same channel, according to eq. (1):

$$\mathbf{D} = \left\{ \sum_{Ch=C_3}^{C_{p2}} |\beta Ch_R - \beta Ch_L| ; \sum_{Ch=C_3}^{C_{p2}} |\mu Ch_R - \mu Ch_L| \right\} \quad (1)$$

The vector $\mathbf{D} \in \mathbb{R}^{Ch*2}$ contains all the absolute values of the comparisons.

The vector **D** is sorted, and the first 4 relevant differences are extracted as pairs: e.g. $p_1=\{\beta C_{3R}, \beta C_{3L}\}$, $p_2=\{\mu C_{4R}, \mu C_{4L}\}$, $p_3=\{\mu C_{p2R}, \mu C_{p2L}\}$, $p_4=\{\beta C_{p1R}, \beta C_{p1L}\}$.

Once the most relevant MRPs and channels are defined, the system statistically analyzes them, as shown via boxplots in Fig.2.c. The other MRPs are discarded. In particular, it extracts four thresholds: two upper thresholds and two lower ones. The first ones are realized by calculating the 75th percentiles of the observation matrix referred to specific MRP and channel for both the movements, e.g. for $\mathbf{OM_\beta}$(Ch)**:** $\mathbf{Th_{UP,R}}$ $\mathbf{Th_{UP,L}} \in \mathbb{R}^S$. Similarly, the last ones are realized by calculating the 25th percentiles of the observation matrix referred to specific MRP and channel for both the movements**:** $\mathbf{Th_{DW,R}}$ $\mathbf{Th_{DW,L}} \in \mathbb{R}^S$.

Overall, 16 thresholds are extracted, 8 $\mathbf{Th_{UP}}$ and 8 $\mathbf{Th_{DW}}$ (2 $\mathbf{Th_{UP}}$ and 2 $\mathbf{Th_{DW}}$ per pair p_i, i=1..4). For each pair p_i the lowest $\mathbf{Th_{UP}}$ and the highest $\mathbf{Th_{DW}}$ are selected as reference thresholds. The system subtracts to the reference $\mathbf{Th_{UP}}$ the discarded one, and do the same thing for the $\mathbf{Th_{DW}}$ ones.

As shown in Fig.2d, the subtractions provide interesting information about the windows in which the differences between the signals on the same channel, but for different movements, are emphasized. From the plot in Fig.2d, the system automatically extracts the windows in which the differences overcome the 30% of the maximum absolute value. For instance, the Fig.2d shows that in the case of βC_3, the optimal temporal windows is the entire trial, while in the case of μC_{p2}, 2 optimal temporal windows can be found: [-450ms → -50ms] ∩ [110ms → 820ms]. On these highly representative windows, the system proceeds to the FE stage.

Features extraction. The FE stage uses the 8 reference thresholds (2 for each pair p_i) and considers only the trial windows provided by the previous ML step.

The FE consists in a kind of EEG barcoding:

1. The algorithm selects the β and μ trials of the same specific labelled observation (e.g. 5th observation – Right hand movement), then it considers only the four relevant signals, as previous stated (e.g. βC_3, μC_4, μC_{p2}, βC_{p1}).
2. The algorithm realizes, on the selected trial (Tr), two barcodes by eq. (2) and (3):

$$\mathbf{bTr_{UP}} = \begin{cases} Tr(i) > Th_{UP}(i) \rightarrow bTr(i) = 1 \;\; i = 1..S \\ otherwise \rightarrow bTr(i) = 0 \end{cases} \quad (2)$$

$$\mathbf{bTr_{DW}} = \begin{cases} Tr(i) < Th_{DW}(i) \rightarrow bTr(i) = 1 \;\; i = 1..S \\ otherwise \rightarrow bTr(i) = 0 \end{cases} \quad (3)$$

3. The resulting signals are sliced in the prescribed temporal windows.
4. After discarding the useless barcode pieces, the system sums all the bits that compose both the barcodes, realizing the feature matrix $\mathbf{f} \in \mathbb{R}^8$.

E. The Classification Models

The 1D vectors **f** are concatenated and labelled (R or L), to realize the train set matrix $\mathbf{F} \in \mathbb{R}^{(Nf+1),No}$, in which each row has the form: {**F**i∈ $\Re^{Nf}$, Li}, where i=1…N_o. N_o is the number of observations, N_f is the number of features (N_f=8) and Li∈ {−1, 1} is the i-th trial label: Yi=-1 → Left hand movement, while Yi= 1 → Right hand movement. The **F** is used

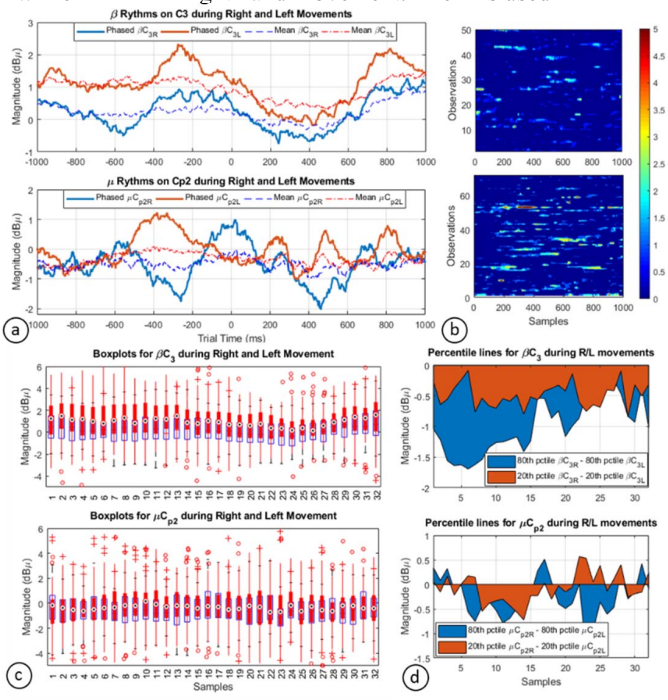

Fig.2 (a) β and μ rhythms on C3 and Cp2 during right (blue lines) and left movements (red lines). (b) OM_μ for the C_{p2} channel during right (top) and left movements (bottom) (c) top: boxplots of βC_3 during right (blue) and left (red) movements. bottom: boxplots of μC_{p2} during right (blue) and left (red) movements. (d) differences between percentile lines.

to train the SVMs [19], with four different kernel bases: linear, quadratic, cubic and Gaussian. Iteratively, a k-folded validated accuracy [19] is performed for each classifier on the train set. The highest accuracy model is selected and uploaded in an extrinsic function on Simulink for the real time classification.

F. The On-line Prediction

In the real-time prediction block, the system extracts the β and μ signals from the FFT radix-2 blocks, then submit them to a coherent down sampling with a rate of 32 (1024 samples →32 samples). When the trigger rising edge occurs, the system extracts the trial, which is, in this case, *unlabeled*. The β and μ trials are submitted to the first dimensionality reduction, managed by the MLE RIDE. It chooses the most relevant MRPs and channels as stated in Sec. III.C.
Eight features are extracted from the unlabeled trials following the steps from 1 to 4 of the Sec. III.C: Feature Extraction. The 1D vector **f** (eq.(4)) feeds the chosen SVM model, which provides in output the command to be actuated.

IV. The Actuators

The SVM classifier sends the predicted label to a dedicated block that manages the Bluetooth communication. Firstly, the Simulink model opens the communication by sending a string: `{89, command, 89}`. The communications are then stopped waiting for the next trigger edge. The HC-05 placed on the actuator is programmed to operate at 9600 baud. In this paper, we propose the Bluetooth-driven actuation of a three-finger robotic hand and an acrylic prototype car, which are shown in Fig.3 with their available functionalities.
The used prototype car is the one largely detailed in our previous work [2].The three-finger robotic hand is a homemade structure, which operates by using three servomotors in tensile or releasing progressions. It operates with three gradual steps in the closing phase and the same number of steps in the opening stage. Thus, using a two choices paradigm is possible to open or close a robotic hand with a self-paced timing [20].

V. Results

The proposed architecture has been tested in vivo on a dataset of 3 subjects (aged 26±1), all students of Politecnico di Bari.
The Table II resumes the composition of the datasets on which the experimental results in the following are based.
In the top tab is shown the train dataset composition in terms of: test typology (Test0 to Test5) in normal and noisy (N) environment [21]. In the table, they are also distinguished by the observation for the right hand movement (R) and left hand ones (L). The bottom tab shows the real-time validation dataset composition, with the same criteria of the train set.
The system accuracy is defined as the ratio between the correctly detected observations (supervised) and the total number of requested actions.

A. Machine Learning Performance

The ML stage is performed off-line through a MATLAB script on a PC equipped with Intel i5 processor and 16GB RAM.
It requests, on average, 11.41±4.6s to perform the signal re-phasing by MLE-RIDE on 4 channels, inference-based

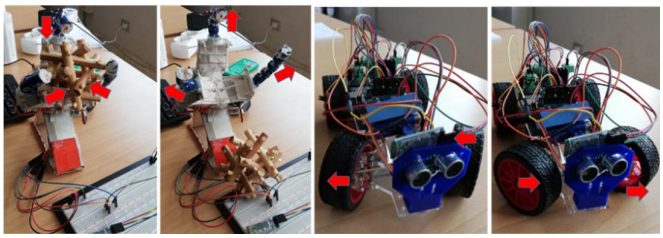

Fig.3 (a) Mechatronic devices Bluetooth interfaced with Simulink based BCI: three-finger robotic hand and acrylic prototype car. (b) Simulink control panel

Features Extraction and SVM model selection. The k-fold (with k=15) validation [14] accuracies for each SVM model, test and subject are shown in Table III.
The table provides information about the implemented SVM models performance in terms of: mean accuracy along the tests, number of support vectors and classification timing. The Cubic SVM ensures the best performance along all the tests with a total accuracy of 91.4±1.23%.
The Test3, which does not require physical interaction with a button, shows the worst performance, with an overall accuracy of the 86.55±2.59% against the 92.23±2.71% of the Test1. Considering the normal and noisy tests separately, the accuracy decreases from an overall value of 93.41% (normal) to 85.62% (noisy). Selecting a specific model (e.g. Cubic SVM on T1, Sub.1) and applying it to all the other tests datasets, the permutations return accuracies that range from a minimum of 71.4% to a maximum of 96.5%.

B. Real-Time Validation

In the real-time validation context, the datasets as reported in Table II has been divided into two equal parts. The first dataset part is dedicated to a mixed commands pattern (R & L) to be actuated on a robotic hand, while the second one on the acrylic prototype car. Fig.4 shows the real time system response in term of accuracy versus test typology, subject and actuator. It shows that, overall, the BCI accuracies when the actuator is the robotic hand and when it is an acrylic car is almost the same: 87.36±0.02%.

C. Classification Timing

In a future perspective of a fast and asynchronous BCI, the proposed system has reserved attention to strict constraints on the computational times for the real time operation [2].

TABLE II . DATASETS COMPOSITION FOR TRAINING AND VALIDATION

Train Datasets Composition													
Sub.	**Age**	**T0**		**T1**		**T2**		**T3**		**T4**		**T5**	
				-	**N**	**-**	**N**	**-**	**N**	**-**	**N**	**-**	**N**
1	25	181	**R**	62	51	81	63	64	52	50	47	52	45
			L	65	44	80	61	66	50	50	48	59	44
2	25	174	**R**	72	45	74	60	66	51	50	36	61	51
			L	70	47	79	60	66	55	50	37	66	50
3	27	166	**R**	61	48	50	42	71	61	50	49	67	49
			L	66	48	52	49	78	62	50	51	71	55
Real-Time Validation Datasets Composition (Prescribed Pattern)													
Sub.	**Age**	**T0**		**T1**		**T2**		**T3**		**T4**		**T5**	
				-	**N**	**-**	**N**	**-**	**N**	**-**	**N**	**-**	**N**
1	25	-	**R**	40	30	40	12	50	25	40	15	40	21
			L	40	30	40	15	50	20	40	12	40	22
2	25	-	**R**	40	30	40	17	50	18	40	13	40	20
			L	40	30	40	19	50	19	40	15	40	19
3	27	-	**R**	40	-	40	-	50	-	40	-	40	-
			L	40	-	40	-	50	-	40	-	40	-

TABLE III . SVM KERNELS COMPARISON

SVM	Linear		Quadratic		Cubic		Gaussian	
Accuracy*1 (%)	*S1*	90.02	*S1*	91.42	*S1*	92.42	*S1*	88.34
	S2	88.06	*S2*	89.44	*S2*	90.04	*S2*	87.40
	S3	89.36	*S3*	89.48	*S3*	91.76	*S3*	89.26
# Support Vectors	*S1*	51	*S1*	62	*S1*	74	*S1*	47
	S2	56	*S2*	64	*S2*	76	*S2*	59
	S3	52	*S3*	61	*S3*	71	*S3*	58
Classification timing*2 (ms)	*S1*	4.16	*S1*	4.54	*S1*	5.26	*S1*	4.24
	S2	4.25	*S2*	4.54	*S2*	5.21	*S2*	4.24
	S3	4.25	*S3*	4.61	*S3*	5.43	*S3*	4.21

*[1]Mean accuracy along the tests (green histograms) *[2]Computed from num. of predictions/s

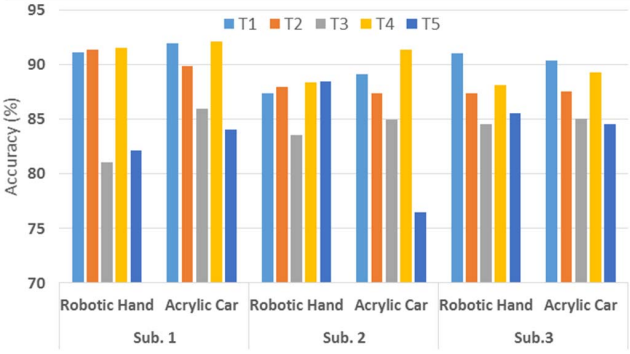

Fig.4 Real time validation accuracy versus test typology, subject and actuator

The system requires a fixed communication latency of 14ms and 1s data after the trigger rising edge. Then, once the data are acquired, the computational chain (FFT + inference-based FE), jointly with the Bluetooth transmission and actuation, asks for 33.7±6.1ms.

VI. CONCLUSIONS

The paper detailed the implementation and test of an MRP-based BCI for the remote control of mechatronic devices. The system, fully implemented on a hybrid platform MATLAB-Simulink, interfaces a wireless EEG headset, which provides the acquisition from 5 channels.

The here presented architecture embeds a novel BCI algorithm that exploits the time-frequency analysis and a statistical inference-based features extraction stage to reduce the training time, and the data needed for the classification, if compared with the current state of the art.

Experimental results obtained on a dataset of 3 subjects provide results that can make the paper a pilot in the study. Indeed, considering a short machine training (~10min) and a small amount of data (only 2s long EEG trial * 5 EEG channels) the system reaches, on average, an accuracy of 87.36±0.02%. The computational chain leads to the user's intention recognition, Bluetooth transmission, and actuation in 33.7±6.1ms. We consider the above strategy giving the direction for further investigations.

REFERENCES

[1] Grychtol, B., Lakany, H., Valsan, G., & Conway, B. A. (2010). Human behavior integration improves classification rates in real-time BCI. Neural Systems and Rehabilitation Engineering, 8(4), 362-368.

[2] D. De Venuto, V. F. Annese and G. Mezzina, "An embedded system remotely driving mechanical devices by P300 brain activity," Design, Automation & Test in Europe Conference & Exhibition (DATE), 2017, Lausanne, 2017, pp. 1014-1019. doi: 10.23919/DATE.2017.7927139

[3] Farwell, L.A., & Donchin, E. (1988). Talking off the top of your head: Toward a mental prosthesis utilizing event-related brain potentials. Electroenceph Clin Neurophysiol, 70(6), 510-523.

[4] Ortner, Rupert, et al. "An SSVEP BCI to control a hand orthosis for persons with tetraplegia." IEEE Transactions on Neural Systems and Rehabilitation Engineering 19.1 (2011): 1-5.

[5] Nijholt, Anton. "BCI for games: A 'state of the art' survey." International Conference on Entertainment Computing. Springer Berlin Heidelberg, 2008.

[6] V. F. Annese, M. Crepaldi, D. Demarchi and D. De Venuto, "A digital processor architecture for combined EEG/EMG falling risk prediction," 2016 Design, Automation & Test in Europe Conference & Exhibition (DATE), Dresden, 2016, pp. 714-719. 978-3-9815-3707-9

[7] Blankertz, B., Curio, G., & Müller, K. R. (2002). Classifying single trial EEG: Towards brain computer interfacing. In Advances in neural information processing systems (pp. 157-164).

[8] N. Birbaumer, N. Ghanayim, T. Hinterberger, I. Iversen, B. Kotchoubey, A. Kübler, J. Perelmouter, E. Taub, and H. Flor, "A spelling device for the paralysed", Nature, 398: 297–298, 1999

[9] B. O. Peters, G. Pfurtscheller, and H. Flyvbjerg, "Automatic Differentiation of Multichannel EEG Signals", IEEE Trans. Biomed. Eng., 48(1): 111–116, 201

[10] Hübner D, Verhoeven T, Schmid K, Müller KR, Tangermann M, et al. (2017) Learning from label proportions in brain-computer interfaces: Online unsupervised learning with guarantees. PLOS ONE 12(4): e0175856. https://doi.org/10.1371/journal.pone.0175856

[11] R. Leeb, L. Tonin, M. Rohm, L. Desideri, T. Carlson and J. d. R. Millán, "Towards Independence: A BCI Telepresence Robot for People With Severe Motor Disabilities," in Proceedings of the IEEE, vol. 103, no. 6, pp. 969-982, June 2015.

[12] M. de Tommaso, E. Vecchio, K. Ricci, A. Montemurno, D. De Venuto and V. F. Annese, "Combined EEG/EMG evaluation during a novel dual task paradigm for gait analysis," 2015 6th International Workshop on Advances in Sensors and Interfaces (IWASI), Gallipoli, 2015, pp. 181-186. doi: 10.1109/IWASI.2015.7184949

[13] V. F. Annese and D. De Venuto, "The truth machine of involuntary movement: FPGA based cortico-muscular analysis for fall prevention," 2015 IEEE International Symposium on Signal Processing and Information Technology (ISSPIT), Abu Dhabi, 2015, pp. 553-558. doi: 10.1109/ISSPIT.2015.7394398

[14] Elaine Marieb, Katja Hoehn, Human Anatomy & Physiology, 7ª, San Francisco, Pearson Prentice Hall, 2007, ISBN 0-13-173297-8.

[15] S. Carrara, M. D. Torre, A. Cavallini, D. De Venuto and G. De Micheli, "Multiplexing pH and temperature in a molecular biosensor," 2010 Biomedical Circuits and Systems Conference (BioCAS), Paphos, 2010, pp. 146-149. doi: 10.1109/BIOCAS.2010.5709592

[16] De Venuto D., Annese V.F., de Tommaso M., Vecchio E., Sangiovanni Vincentelli A.L. (2015) Combining EEG and EMG Signals in a Wireless System for Preventing Fall in Neurodegenerative Diseases. In: Andò B., Siciliano P., Marletta V., Monterià A. (eds) Ambient Assisted Living. Biosystems & Biorobotics, vol 11. Springer, Cham

[17] V. F. Annese and D. De Venuto, "FPGA based architecture for fall-risk assessment during gait monitoring by synchronous EEG/EMG," 2015 6th International Workshop on Advances in Sensors and Interfaces (IWASI), Gallipoli, 2015, pp. 116-121. doi: 10.1109/IWASI.2015.7184953

[18] D. De Venuto, V. F. Annese and G. Mezzina, "Remote Neuro-Cognitive Impairment Sensing Based on P300 Spatio-Temporal Monitoring," in IEEE Sensors Journal, vol. 16, no. 23, pp. 8348-8356, Dec.1, 2016. doi: 10.1109/JSEN.2016.2606553

[19] Kecman V., T. -M. Huang, and M. Vogt. "Iterative Single Data Algorithm for Training Kernel Machines from Huge Data Sets: Theory and Performance." In Support Vector Machines: Theory and Applications, 255–274. Berlin: Springer-Verlag, 2005.

[20] V. F. Annese and D. De Venuto, "Fall-risk assessment by combined movement related potentials and co-contraction index monitoring," 2015 IEEE Biomedical Circuits and Systems Conference (BioCAS), Atlanta, GA, 2015, pp. 1-4. doi: 10.1109/BioCAS.2015.7348366

[21] D. De Venuto and E. Stikvoort, "Low Power High-Resolution Smart Temperature Sensor for Autonomous Multi-Sensor System," in IEEE Sensors Journal, vol. 12, no. 12, pp. 3384-3391, Dec. 2012. doi: 10.1109/JSEN.2012.21989